Journal of Japan Association for Earthquake Engineering, Vol. 21, No. 3, 2021

DEEP SUBSURFACE S-WAVE VELOCITY STRUCTURE OF OKINAWA ISLANDS, JAPAN —FOR NUMERICAL MODELING

Nobuyuki YAMADA[1] and Hiroshi TAKENAKA[2]

[1] Member, Assoc. Prof., Dept. of Global Environment and Disaster Prevention, Kochi University, Kochi, Japan, nyamada@kochi-u.ac.jp
[2] Member, Professor, Dept. of Earth Sciences, Okayama University, Okayama, Japan, htakenaka@cc.okayama-u.ac.jp

ABSTRACT: In this paper, we report the results of an analysis using microtremor array data to estimate a 1D S-wave velocity structure consisting of several layers and an S-wave 3 km/s layer around the Okinawa Islands. The depths of the top of S-wave 3 km/s layer at each site are 0.2 to 0.4 km in northern and western Okinawa Island and Kume Island, and 2.0 to 2.5 km in southern Okinawa Island. The average S-wave velocities of each layer (0.69, 1.10, 2.01, and 3.46 km/s) and the depth of the layer boundary are also presented for the four-layer model based on the estimation results for all locations.

Keywords: Okinawa Islands, S-wave velocity structure, Microtremor array exploration

1. INTRODUCTION

The Okinawa Islands, located in the center of the Nansei Islands, consist of Okinawa Island, Kerama Islands, Iheya–Izena Islands, Kume Island, and other islands. These areas, especially the southern part of Okinawa Island where the prefectural capital Naha City is located, which is also a densely populated area, needs to be prepared not only for typhoons but also for seismic disasters. According to the Headquarters for Earthquake Research Promotion[1)], there have been reports of damage caused by M7 class earthquakes in the vicinity of the Okinawa Islands. In 2010, the M7.2 earthquake off the east coast of Okinawa Island caused a JMA seismic intensity of 5-lower in Itoman City in the southern part of Okinawa Island, and a JMA seismic intensity of 4 in Naha City and a wide area, resulting in injuries and damage to houses and historical buildings throughout Okinawa Island (e.g., Fire and Disaster Management Agency[2)], Nakamura et al.[3)]). According to the Strong-motion Prediction Map (The Headquarters for Earthquake Research Promotion[4)]), there is a high possibility that Naha and other coastal areas of southern Okinawa Island will be hit by strong motions in a huge earthquake of the Ryukyu Trench or the Okinawa Trough. In addition, considering the historical background of the area has not been hit by strong ground motions for several decades since the end of the war in the 1940s there

are probably buildings in the area with seismic resistance problems (e.g., Kashima and Ono[5]). In the eastern part of Okinawa Island, there are some structures that need to be evaluated with regard to long-period ground motion, such as the national oil storage base. Therefore, it is important to improve the accuracy of the velocity structure model that can be applied to the evaluation of a wide period range of ground motion to mitigate seismic disasters in the Okinawa Islands.

The S-wave velocity (Vs) structure is one of the most important parameters in seismic motion evaluation. The deep subsurface structure model to the top of the layer with S-wave velocity of approximately 3 km/s has been available at the J-SHIS (National Research Institute for Earth Science and Disaster Resilience[6]) since 2014 for the area around the Nansei Islands. In the sea around this area, large-scale subsurface investigations have been carried out (e.g., Nishizawa et al.[7]) and island geological surveys (e.g., Nakae[8]) and borehole investigations of several hundred to one thousand meters have been carried out, mainly on the island of Okinawa (e.g., Leroy[9]). Deep boreholes and seismic explorations have been conducted in the southern part of Okinawa Island to investigate resources such as hot springs and natural gas (e.g., Okinawa Prefecture[10]). However, these borehole surveys only show the depth of the geological boundary and do not provide information on the velocity structure or PS logging. In previous studies, there is little geophysical information on which to base the physical properties of the subsurface structure models required for seismic motion evaluation. In addition, the J-SHIS model did not contain sufficient information to prepare base for the velocity structure model.

Our studies have conducted microtremor array observations in the long-period ground motion from approximately 0.5 to several seconds for deep subsurface structure exploration in the Nansei Islands, Yamada and Takenaka[11] have summarized the velocity structure of the islands of the Miyako and Yaeyama Islands. In this paper, we report the results of the estimation of deep subsurface S-wave velocity structure from the layer of Vs 0.6 km/s to the layer of Vs 3.0 km/s in the Okinawa Islands. In addition, the results of the process of building a numerical model for ground motion evaluation are also described. The target islands are Okinawa Island and its surrounding small islands, Kume Island and Zamami Island, and some of the survey points are adjacent to the seismic stations of the National Research Institute for Earth Science and Disaster Prevention and the Japan Meteorological Agency. These results show the 1D S-wave velocity structure at a point on the islands scattered in the Nansei Islands; however, it is expected to be an important parameter for improving the accuracy of the 3D subsurface structure model of the area.

2. OUTLINE OF THE TOPOGRAPHY AND GEOLOGY OF THE OKINAWA ISLANDS

Figure 1a shows the location of the Okinawa Islands, and Fig. 1b shows the topography (Geospatial Information Authority of Japan[12]) in color contours. Okinawa Island, the largest island of these islands is located about 300 km northeast of Miyakojima in the Sakishima Islands and about 150 km southwest of Amami Oshima in the Amami Islands, and it has an elongated shape of approximately 100 km from north to south and about 5–30 km from east to west. The topographic and geological characteristics of Okinawa Island differ between the northern and southern regions (the thick black dotted line in Fig. 1b is the border). The topography of Okinawa Island is such that it is mountainous in the north with an altitude of 300–400 m and few plains, whereas the south has many plateaus and lowlands less than 100 m above sea level. In this island's surface geology, the northern part of the area is dominated by older sediments (300 million to 50 million years old), whereas the southern part of the area is dominated by younger sediments (after 5 million years old) such as the Shimajiri Group and Ryukyu Limestone (Shinshiro[13]). According to the geological map, the surface geology of Zamami Island, located off the west coast of Okinawa Island, is similar to that of northern Okinawa Island, whereas that of Kume Island is Cenozoic volcanic rocks and limestone (Geological Survey of Japan, National Institute of Advanced

Industrial Science and Technology: Geomap Navi[14]).

In the southern part of Okinawa Island, several boreholes have been drilled down to approximately 1000 m for geological, oil, and natural gas investigations (e.g., Fukuda et al.[15]), and the geological boundary depth was indicated. Fig. 2a shows the locations of previous borings. The points for which the details of the boring location in the references were not indicated, were read from the map in corresponding references. According to Fig. 2a, the boring locations are arranged in a northwest–southeast direction from the vicinity of Naha City, and a summary of these investigations is shown in Table 1. Nanjo R-1 was drilled in 2009, Naha R-1 and Osato R-1 in 2014, and the others were drilled from the 1950s to the 1970s; their paleontological and geochemical analyses and interpretations were carried out recently (e.g., Okinawa Prefecture Industrial Policy Division, Industrial Policy Division, Department of Commerce, Industry and Labor, Okinawa Prefectural Government[16]). The values of the boundary depth of each layer in Table 1 are those described in the references or read from the figures. In Table 1, "Non" was used in case of no mention of the existence of the corresponding layer in the references, and "?" was used in cases where the details were unknown. In each reference, the Ryukyu limestone, Niizato formation, Yonabaru formation, and Tomigusuku formation are described from the surface, and the pre-Tertiary Nago formation is referred to as the basement rock. When the drilling depth of the boreholes was shallower than the depth of the Nago formation, the depth of the basement was indicated to be greater than the drilling depth. In Table 1, the depth contour map of the top of the basement rock at 100 m intervals from the seismic exploration (Okinawa Prefecture[10]) results by Kato et al. were read, and the values are described. Based on the values in Table 1, the boundary depth values at RS2 to NJ1 and RS2 to GS1 for aligned northwest–southeast are plotted in Fig. 2b. RS1 and RS3 are the median values of the range of readings. The depth of the upper Nago formation in RS2 and NH1 on the northwest side is approximately 1000 m, whereas that in NJ1 on the southeast side is approximately 2000 m. This suggests that the Nago formation is tilted in a northwest–southeast direction. A similar northwest–southeast trending structure is inferred for the boundaries of the Tomigusuku and Yonabaru formations above it. Furthermore, the gravity map (Bouguer anomaly) of Geomap Navi[14] shows a decreasing contour from Kume Island through the northwestern part of Okinawa Island to the southeast, with the smallest values near the southeastern part of Okinawa Island. The two trends are similar under the assumption that the change trend in the gravity map reflects the change in the depth of the geological boundary.

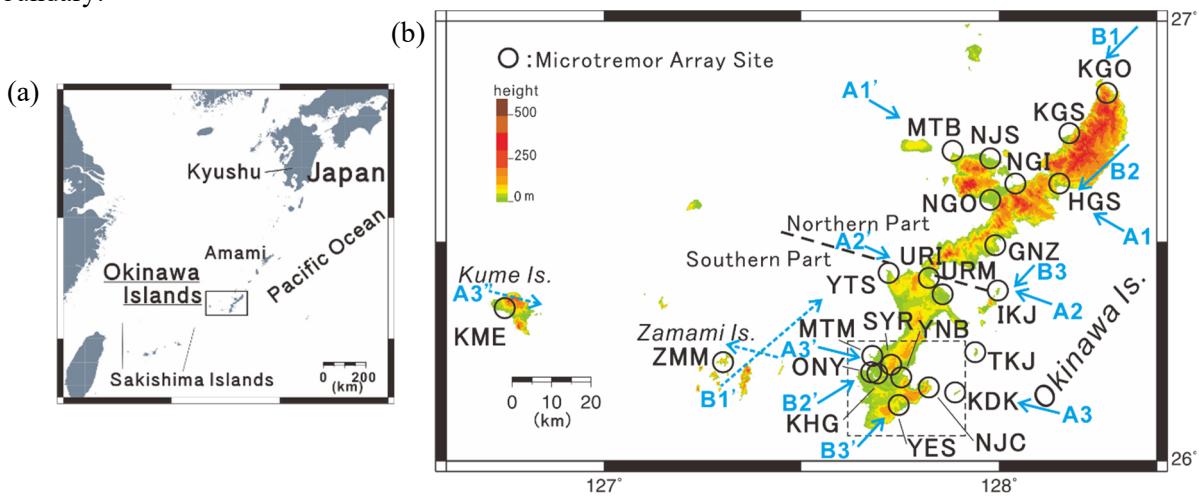

Fig. 1 (a) Location of the Okinawa Islands, the square box represents the target area of this study in Fig. 1b (b) Map of the microtremor array location (○), the thin dotted rectangle represents the area in Fig. 2a, the light blue lines A1–A1' to A3–A3' and B1–B1' to B3–B3' indicate the positions of the measurement lines shown in Fig. 8

Table 1 Layer boundary depths described in previous drilling studies (unit: m)

Geological age(upper/lower)	Petrostratigraphy(upper/lower)	RS2	NH1	RS1	YB1	OZ1	NJ1	RS3	GS1
Quaternary/Neogene : Pliocene	Ryukyu Limestone/Niizato	17.0	Non	?	?	Non	5.0	?	18.5
Pliocene/Pliocene	Niizato/Yonabaru	Non	Non	?	?	Non	Non	?	105.0
Pliocene/Miocene	Yonabaru/Tomigusukur	Non	Non	185.0	*	390.0	725.0	260.0	1003.0
Miocene/Pre-Tertiary	Tomigusuku/Nago	935.8	980.0	>435	>1230	1547.0	1972.0	>1010	>1709
	Drilling depth (m)	978.38	1243.0	435.0	4036(ft.)	1800.0	2119.49	1010.0	1708.65
	Reference number	16), 17)	16), 17)	10), 19)	9),18),19)	16), 17)	17), 20)	18), 19)	17), 21)
The top depth of basement on contour map by reference 17). (m)		900-1000	900-1000	1200-1300	1300-1400	1500-1600	1800-1900	1500-1600	?

*: Description of the Yonabaru Layer only

Table 2 Summary of the information of microtremor array observation

No.	Site name	Code	Lon. (°)	Lat. (°)	Height (m)	Year/Month /Day	Record start time (duration: min.)	Instrument interval(m) Min. - Max.	*
1	Kunigamison Oku	KGO	128.2737	26.8378	230	2015/9/29	10:00(30), 11:15(60)	49 - 863	3
2	Kunigamison	KGS	128.1777	26.7455	4	2009/2/11	15:00(60), 17:00(30)	38 - 923	1
3	Motobu	MTB	127.8821	26.7060	4	2016/11/5	10:05(30), 10:55(30)	45 - 343	3
4	Nakijinson	NJS	127.9791	26.6903	26	2015/9/29	14:35(30), 15:30(60)	52 - 1273	3
5	Nago Inamine	NGI	128.0418	26.6331	10	2016/11/4	13:45(30), 14:58(60)	55 - 977	3
6	Higashison	HGS	128.1514	26.6324	6	2016/11/4	10:40(30), 11:40(60)	53 - 875	3
7	Nago	NGO	127.9786	26.5949	9	2014/2/19	11:10(60), 13:00(30)	58 - 1138	3
8	Ginoza	GNZ	127.9915	26.4925	44	2015/9/30	12:25(30), 13:20(60)	66 - 1378	3
9	Yomitan	YTS	127.7214	26.4289	22	2015/9/30	8:55(30), 9:50(60)	66 - 1225	3
10	Uruma Ishikawa	URI	127.8235	26.4184	38	2016/11/5	14:15(30), 15:25(60)	98 - 1005	3
11	Ikejima	IKJ	127.9960	26.3905	18	2015/9/28	12:15(30), 13:15(45), 14:30(60)	48 - 1314	3
12	Uruma	URM	127.8583	26.3797	19	2014/2/20	10:45(30), 12:00(60)	40 - 849	3
13	Tsukenjima	TKJ	127.9394	26.2483	15	2016/11/6	10:30(60), 12:30(45), 13:40(30)	57 - 1243	3
14	Naha Minatomachi	MTM	127.6787	26.2416	3	2009/11/19 2010/2/23	17:30(60) 22:00(30)	75 - 1129	2
15	Naha Syuri	SYR	127.7259	26.2218	116	2009/11/21 2010/3/1	14:00(30) 13:00(60)	68 - 659	2
16	Naha Ohnoyama	ONY	127.6757	26.2022	3	2009/11/20	15:30(30), 16:30(60)	77 - 810	2
17	Naha Kohagura	KHG	127.6930	26.2010	24	2009/11/20	7:00(30), 8:00(60)	37 - 765	2
18	Yonabaru	YNB	127.7522	26.1924	29	2012/3/6	14:55(60), 16:32(30), 17:20(20)	50 - 1298	3
19	Nanjyo Chinen	NJC	127.8213	26.1697	81	2009/2/15	3:00(60), 5:00(30)	58 - 813	1
20	Kudakajima	KDK	127.8880	26.1587	12	2012/3/6	10:15(60), 11:45(30), 12:25(15)	24 - 997	3
21	Yaese	YES	127.7450	26.1301	76	2015/10/1	11:10(30), 12:10(45), 13:15(60)	64 - 1377	3
22	Kume Island	KME	126.7480	26.3496	28	2010/2/28	15:45(30), 17:15(60)	97 - 1044	2
23	Zamami Island	ZMM	127.3029	26.2273	4	2010/11/23	11:30(30), 13:00(60)	74 - 1072	2

*: Recorder: 1 = LS8000-SH (16 bit), 2 = LS8000-WD (24 bit), 3 = LS8800 (24 bit)

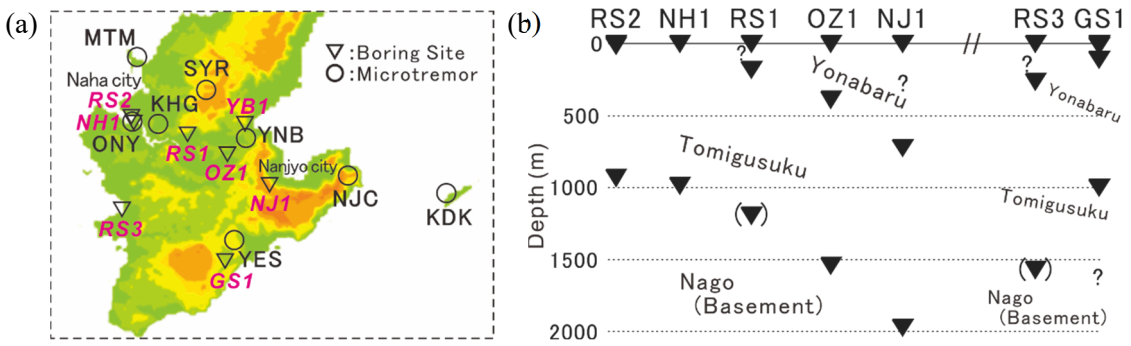

Fig. 2 (a) Borehole survey points in southern Okinawa Island (b) Plots of layer boundary depth

Photo 1 Example of the photo during microtremor observation at HGS

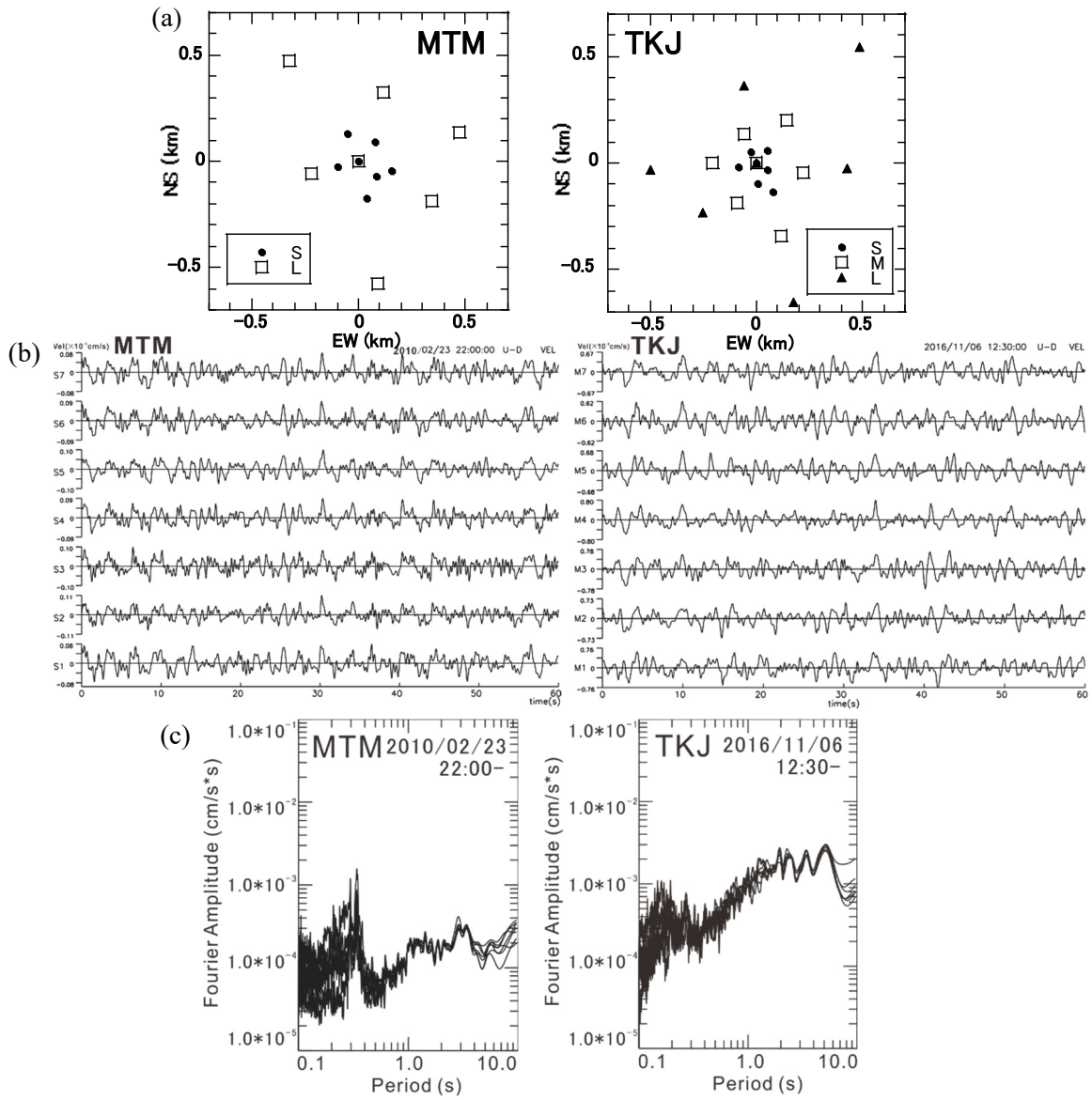

Fig. 3 (a) Example of instrument arrangement in MTM and TKJ for microtremor array observation (b) Examples of microtremor velocity waveforms obtained from MTM and TKJ observations (after band-pass filter for periods of 0.3 to 10.0 s) (c) Example of a velocity Fourier spectrum for the time containing the data in Fig. 3b (about 82 s)

3. MICROTREMOR ARRAY OBSERVATION

In this study, we carried out microtremor array observations to clarify the S-wave subsurface velocity structure at the target sites. The survey sites are represented by the circles in Fig. 1b. A total of 23 sites were surveyed, out of which 18 sites were on Okinawa Island, and small islands adjacent to the island, furthermore IKJ, TKJ, KDK, ZMM, and KME around Okinawa Island. Most of these points are located near the seismic observatory of K-NET and F-net of the National Research Institute for Earth Science and Disaster Resilience, and the station of seismic and tsunami detection network of the Japan Meteorological Agency. The details of the methods and observations of microtremor arrays and the estimation of the velocity structure are the same as in Yamada and Takenaka[11].

Figure 3a shows an example of the equipment layout in MTM and TKJ. Photo 1 shows an example of the equipment at the microtremor observation point. As shown in Fig. 3a, a total of seven instruments were installed at the apex of the triangle, near the center of gravity (origin position in Fig. 3a), and near the midpoint of each side for simultaneous recording of microtremors. This observation was performed several times by changing the arrangement of the remaining six instruments without changing the position around the center of gravity. The configuration of the arrays varied depending on the conditions of the investigation site. Table 2 provides some information about the array observations. The latitudes and longitudes in Table 2 correspond to the locations near the center of gravity of the array. The length of the observation time was set to 30 to 60 min, and the interval between observation points was set to several tens of meters to 1300 meters, depending on the situation at each site. The equipment used for the simultaneous observations was an over-damped moving coil accelerometer (SMAR-6A3P: 0.3 to 50.0 Hz flat response) by Akashi Corporation and a data logger (recorder shown in Table 2) manufactured by Hakusan Corporation. A 300× internal amplifier was used for the recorder 1 in Table 2, and a 500× external amplifier was used for recorders 2 and 3 in Table 2. All observations were made with a 100 Hz sampling. The internal clocks of the loggers were calibrated with GPS signals to maintain the time difference between the devices less than 1/100 s. In addition, a handheld GPS was used to acquire the location information, and the error was maintained within a few meters.

As described above, the vertical component acceleration records obtained from microtremor observations at various locations were numerically integrated and converted into velocity waveforms (Fig. 3b) for analysis. Examples of the velocity Fourier spectra at MTM and TKJ are shown in Fig. 3c. These sites are located at the western and eastern ends of the southern part of Okinawa Island, and the microtremors were recorded at each other times. The spectra in Fig. 3c were both shaped without any prominent peaks. For periods of 0.5 s or less, the spectra are prone to variation due to human activity around the observation point. For example, MTM is located near the center of Naha City and is considered easily affected by human activity; however, according to Figs. 3b and 3c, the variation is small and the effect is considered to be small. In the records obtained from these simultaneous observations, the spectral records were well aligned at all locations. Therefore, there was no significant difference in the spectral characteristics between the installation points in the same array observation, and it was judged that the data could be fully utilized for the subsequent analysis. Similar results were obtained for the other sites, although there were some differences.

4. ESTIMATION OF PHASE VELOCITY

The microtremor records obtained from the observations described in Section 3 were divided into data sets of 81.92 s and 163.84 s, and processed. The subsequent microtremor data handling and processing followed the process described by Yamada and Takenaka[11]. The data used in the analysis exclude portions of the records that appear to be significantly affected by human activities. For each dataset,

frequency–wavenumber spectrum analysis (Capon[22]) was used to calculate the phase velocity from the wavenumber vector at the peak position of the wavenumber spectrum at each frequency, and the average value of the phase velocity for each dataset was used as the final value. These operations were carried out for each period, and the upper limit of the maximum wavelength for each period was set to five to six times the maximum value of the installation point interval (Table 2) for the same array (e.g., Okada[23]), and a value was adopted so that the velocity values obtained for each array would be continuous to some extent. The phase velocities obtained in this manner for each point are shown in Fig. 4. They show a dispersive property in which the phase velocity becomes larger as the period becomes longer. The phase velocities are considered to be Rayleigh wave phase velocities because the records of vertical motion components are used in the analysis. The obtained phase velocities ranged from approximately 0.5 km/s to 3.0 km/s. In addition, the period range is wide (0.5 to 3.0 s) in the southern part of Okinawa Island (YNB, NJC, KDK, YES) and in IKJ and TKJ on the east side of Okinawa Island, intermediate (0.5 to 2.0 s) in four points in Naha City (MTM, SYR, ONY, KHG), and narrow (0.5 to 1.0 s) in the northern part of Okinawa Island and Kume Island. In general, the slope of the dispersion curve tends to decrease from the northwest to the southeast. The southern part of Okinawa Island, where the phase velocities were obtained in a relatively wide band, is an area of relatively new geology, whereas the northern part of Okinawa Island, where the phase velocities were obtained in a narrow band, is an area of old geology.

Because the frequency–wavenumber spectrum method is used to calculate the phase velocity, the direction of arrival of microtremors can also be calculated. Examples of arrival directions for the MTM and TKJ are shown in Fig. 5. Although each period shows arrivals from various directions, for example, the TKJ cases with periods of 1.8 and 2.6 s show a slightly biased tendency to show arrivals from the northeast and southwest directions. TKJ is a small island off the coast of Okinawa Island and the survey site is very close to the sea in all directions, making sea wave effects possible; however, the exact cause of this trend is unknown.

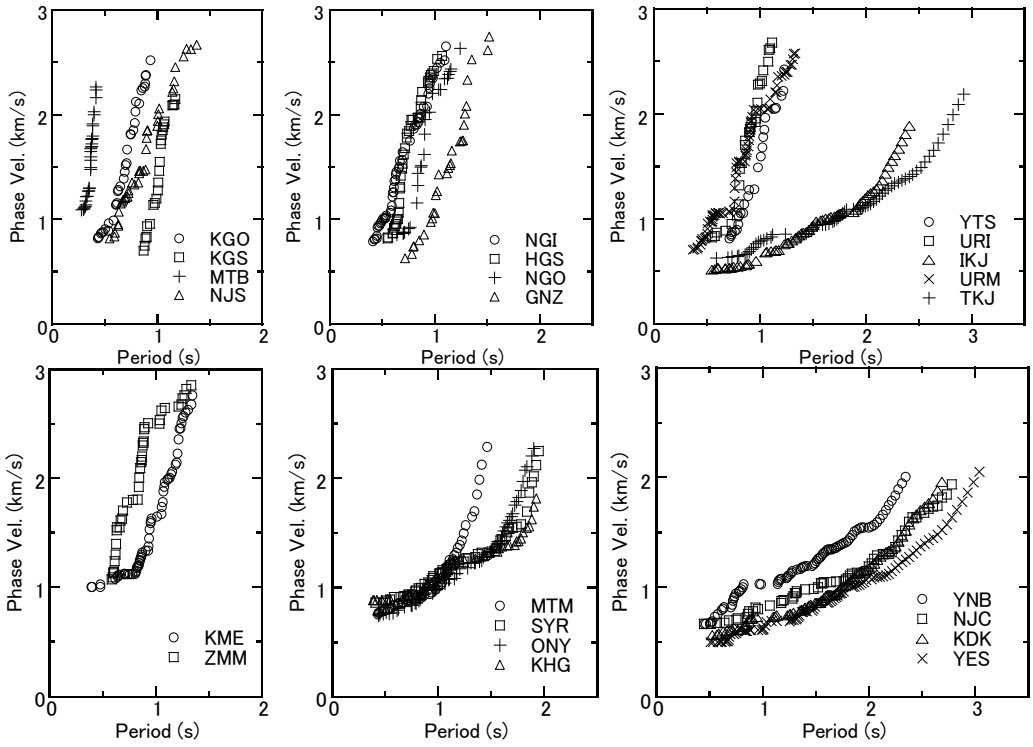

Fig. 4 Phase velocity of Rayleigh waves for every period obtained at each site

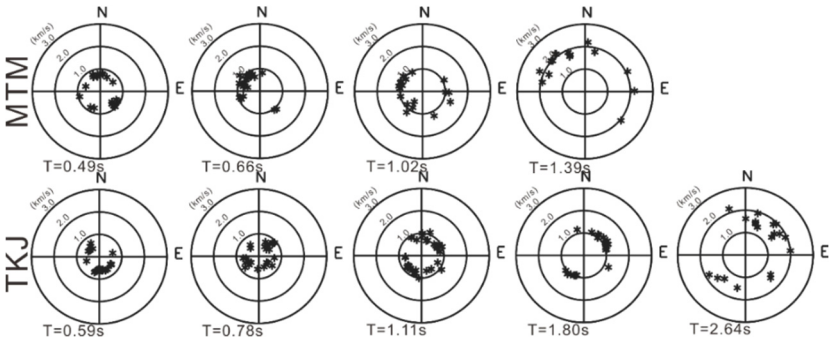

Fig. 5 Example of arrival direction of microtremors, '*' indicates the direction of arrival

5. ESTIMATION OF S-WAVE VELOCITY STRUCTURE

Based on the phase velocities obtained from the microtremor observation records (Fig. 4), the 1D S-wave velocity structure at each site was estimated by inversion using a genetic algorithm (Yamanaka and Ishida[24]). In the inverse analysis, the fundamental mode of the Rayleigh wave is assumed. Then, the average of the models that fit within a range of 1.03 times the minimum of the sum of the absolute values of the differences between the observed and theoretical phase velocities for each cycle (misfit) was searched as the optimal model (Yamanaka and Yamada[25]). For the parameters of the inversion, we set the number of individuals to 20, crossover probability to 70 %, mutation rate to 1 %, and number of generations to 100, similar to Yamanaka et al.[26]. The parameters to be optimized were the Vs value and layer thickness of each layer, and the search for unknowns in each layer was discretized in 8 bit binary numbers. Regarding the setting of the search range of the model during the inversion, the number of layers was set by referring to the fact that the velocity structures shown in J-SHIS were two to four layers with velocity values of 0.6, 1.1, 1.7, 2.1, 3.1, and 3.3 km/s. The 2–4 layer structure was set by trial and error, using the slope of the phase velocity in Fig. 4 and the trend of the periodic band of the phase velocity obtained as references. For the S-wave velocity values, a wide range of values was set around the velocity values for each layer shown in the J-SHIS model to provide a range of estimations. The layer thicknesses were set at 0.001 km to 1.0 km or 2.0 km. Density is the value given in the J-SHIS model. The parameters used are listed in Table 3.

Figure 6 shows the estimated S-wave velocity structure (with the ground surface set at 0 km). The gray line represents all models from the inversion that have an error less than or equal to 1.03 times the minimum value of misfit, and the solid red line (we call this "1st inv.") is the mean value. There are some sites where only a small number of models were adopted as acceptable (ONY, NJC: nine models, NGO, YNB: 11 models), whereas other sites generally adopted more than 20 models. For KGS and URM, the variability is rather large, especially for MTM, and the accuracy of the model is considered to be lower than that of other sites; however, for many sites, the variation of S-wave velocity values and layer thickness values for each layer (gray line spread) is small.

The estimated Vs values and boundary depth of each layer are listed in Table 4. This result is "1st inv". The overall trend of Vs values was 0.5–0.9 km/s in the first layer near the surface and 3.1–3.6 km/s in the lowest layer. Although there are some points where the Vs value is slightly larger, the layer with Vs values of 3.1 to 3.6 km/s corresponds to the seismic basement. For the intermediate layer, the values ranged from 0.9 to 1.6 km/s and 1.6 to 2.4 km/s, respectively. The minimum depth on the seismic basement was approximately 0.2 km (MTB) and the maximum was 2.4 km (YES). The regional trend of these velocity structures is approximately two layers consisting of a seismic basement layer and one layer in the northern part of Okinawa Island from KGO and KGS to YTS and URI, where Vs values of about 1 km/s and layer thicknesses of 0.1–0.4 km were obtained for the first layer. In the southern part

of Okinawa Island, from URM and IKJ to KDK and YES, the model is a four-layer (partly three-layer) model consisting of seismic basement and three layers (partly two layers). The depth to the top of the seismic basement exceeds 2 km in the eastern part, including IKJ, TKJ, and KDK, and the maximum depth is approximately 2.5 km in the YES at the southern end. In addition, the results from MTM, ONY, YNB, NJC, and KDK, which are located from west to east, show that the seismic basement tends to be deeper in the east. The boring results shown in Fig. 2 and the results of this study are not comparable because of the different number of layers; however, they are consistent with the trend that the depth of the lowermost and intermediate layer boundaries gradually deepens from west to east. For ZMM and KME, a two-layer model similar to that of the site in northern Okinawa Island was estimated.

Figure 7 shows a comparison between the theoretical phase velocity of Rayleigh waves (1st inv.: solid red line) calculated from the S-wave velocity structure model in Fig. 6 and the observed phase velocity (obs.). The observed phase velocities in Fig. 7 are also plotted with error bars indicating the variation. The P-wave velocity in the calculation of the theoretical dispersion curve is linked to Vs using the existing empirical formula (Kitsunezaki et al. [27]). Fig. 7 shows that the theoretical phase velocities at most of the sites are within the error bars of the observed values at each frequency, and there is an approximate correspondence between the observed and theoretical phase velocities. Therefore, the S-wave velocity structure estimated in this study is one of the solutions (models) that can calculate the theoretical dispersion curve that fits the observed phase velocity. However, there are differences from the observed values in the period of approximately 1 s in the URI and KGS, suggesting that there is room for modification in the setting of the parameters in the inversion analysis.

The velocity structure model shown in Fig. 6 also includes the deep subsurface structure (dotted line) for each standard regional mesh in the J-SHIS. The S-wave velocity structure estimated in this study is different from the S-wave velocity structure shown in J-SHIS for most of the sites, except for GNZ and ZMM. In the southern part of Okinawa Island, where the depth to the top of the seismic basement was close to 2 km, the Vs values were mostly the same, but the boundary depths were different, and the depths tended to be greater in general. The theoretical phase velocity calculated from the J-SHIS model (gray dotted line) is also shown in Fig. 7, although there are many points where the difference from the observed phase velocity is significant.

Table 3 Search range set in the inversion for 1st inv.

Layer	Vs (km/s)	Th (km)	ρ (g/cm^3)
1	0.8–2.5	0.001–1.0	2.00
2	2.3–3.6	∞	2.60

KGO, MTB, NJS, YTS, URI, KME, ZMM

Layer	Vs (km/s)	Th (km)	ρ (g/cm^3)
1	0.4–1.6	0.001–1.0	2.00
2	1.4–2.5	0.001–2.0	2.35
3	2.3–3.6	∞	2.60

KGS, NGI, HGS, NGO, GNZ

Layer	Vs (km/s)	Th (km)	ρ (g/cm^3)
1	0.4–0.9	0.001–1.0	1.95
2	0.8–1.6	0.001–1.0	2.15
3	1.4–2.5	0.001–2.0	2.35
4	2.3–3.6	∞	2.60

IKJ, URM, TKJ, MTM, SYR, ONY, KHG, YNB, NJC, KDK, YES

Table 4 S-wave velocity structure at each site (Vs: km/s, D: depth in km) obtained by 1st inv.

	KGO		KGS		MTB		NJS		NGI		HGS		NGO		GNZ		YTS		URI		IKJ		URM	
Layer	Vs	D	Vs	D	Vs	D	Vs	D	Vs	D	Vs	D	Vs	D	Vs	D	Vs	D	Vs	D	Vs	D	Vs	D
1									0.78	0.22					0.51	0.18					0.54	0.28	0.56	0.11
2	1.01	0.34	0.99	0.46	1.03	0.18	0.93	0.37			1.00	0.33	1.05	0.43			0.90	0.40	0.94	0.37	1.03	1.03	1.04	0.32
3			1.93	0.52					2.04	0.23	1.80	0.35	2.35	0.45	1.69	0.20					2.42	1.80	2.19	0.48
4	3.52	–	3.44	–	3.49	–	3.56	–	3.57	–	3.57	–	3.58	–	3.57	–	3.45	–	3.53	–	3.15	–	3.54	–

	TKJ		MTM		SYR		ONY		KHG		YNB		NJC		KDK		YES		KME		ZMM	
Layer	Vs	D	Vs	D	Vs	D	Vs	D	Vs	D	Vs	D	Vs	D	Vs	D	Vs	D	Vs	D	Vs	D
1	0.72	0.46	0.83	0.31	0.85	0.31	0.76	0.28	0.90	0.37	0.65	0.19	0.65	0.25	0.65	0.40	0.60	0.37				
2	1.22	1.38	1.26	0.64	1.37	1.01	1.17	0.73	1.42	1.24	1.18	0.83	1.02	0.91	1.13	1.13	1.09	1.19	1.12	0.54	0.88	0.27
3	2.40	2.34	2.08	1.01	1.52	1.21	1.67	1.23	2.26	1.59	1.85	1.86	1.68	1.78	2.20	2.06	2.03	2.38				
4	3.51	–	3.38	–	3.54	–	3.55	–	3.34	–	3.53	–	3.01	–	3.30	–	3.42	–	3.53	–	3.59	–

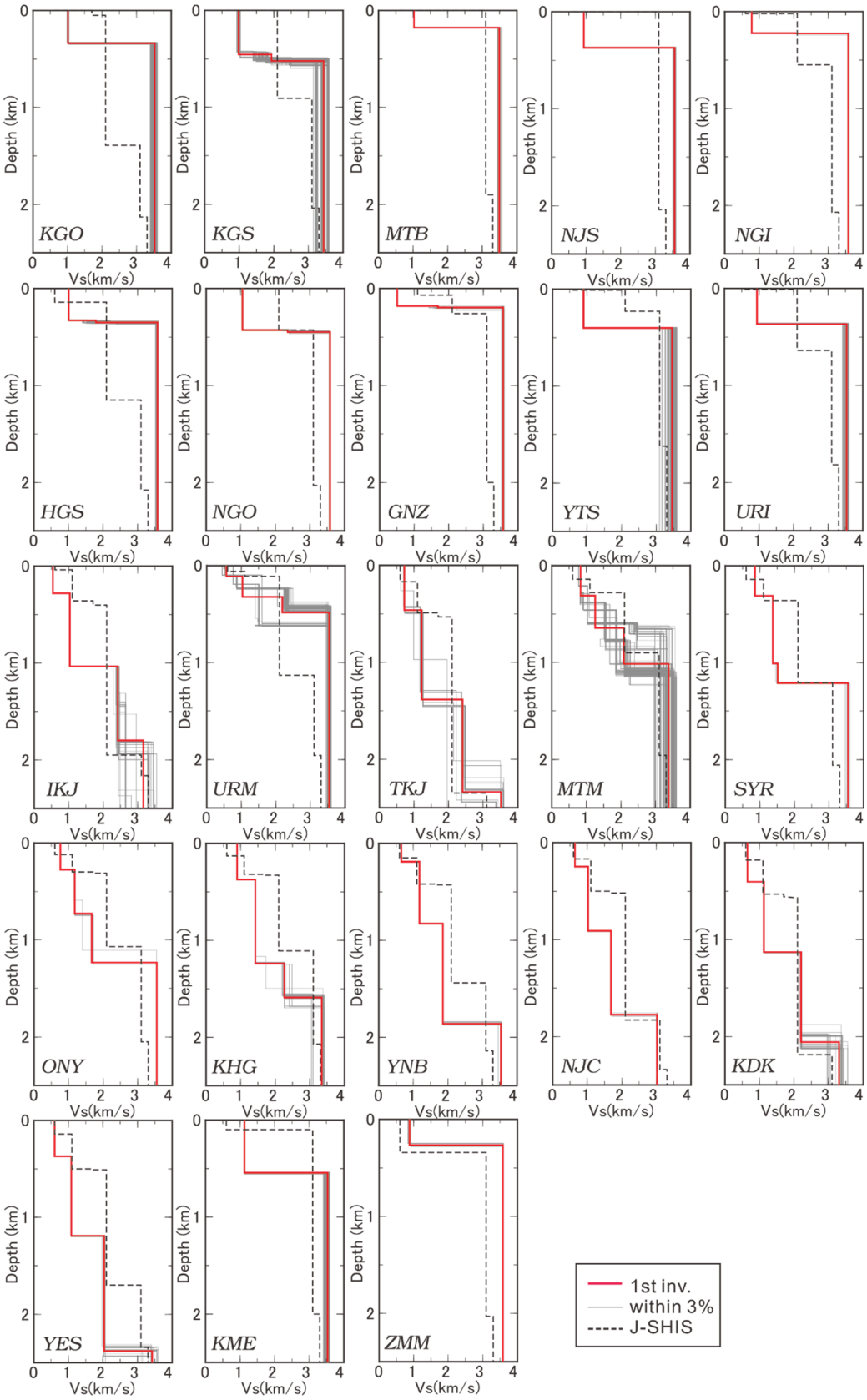

Fig. 6 Velocity structure models (models within 1.03 times the minimum misfit: gray and their average: red; J-SHIS model: dotted line)

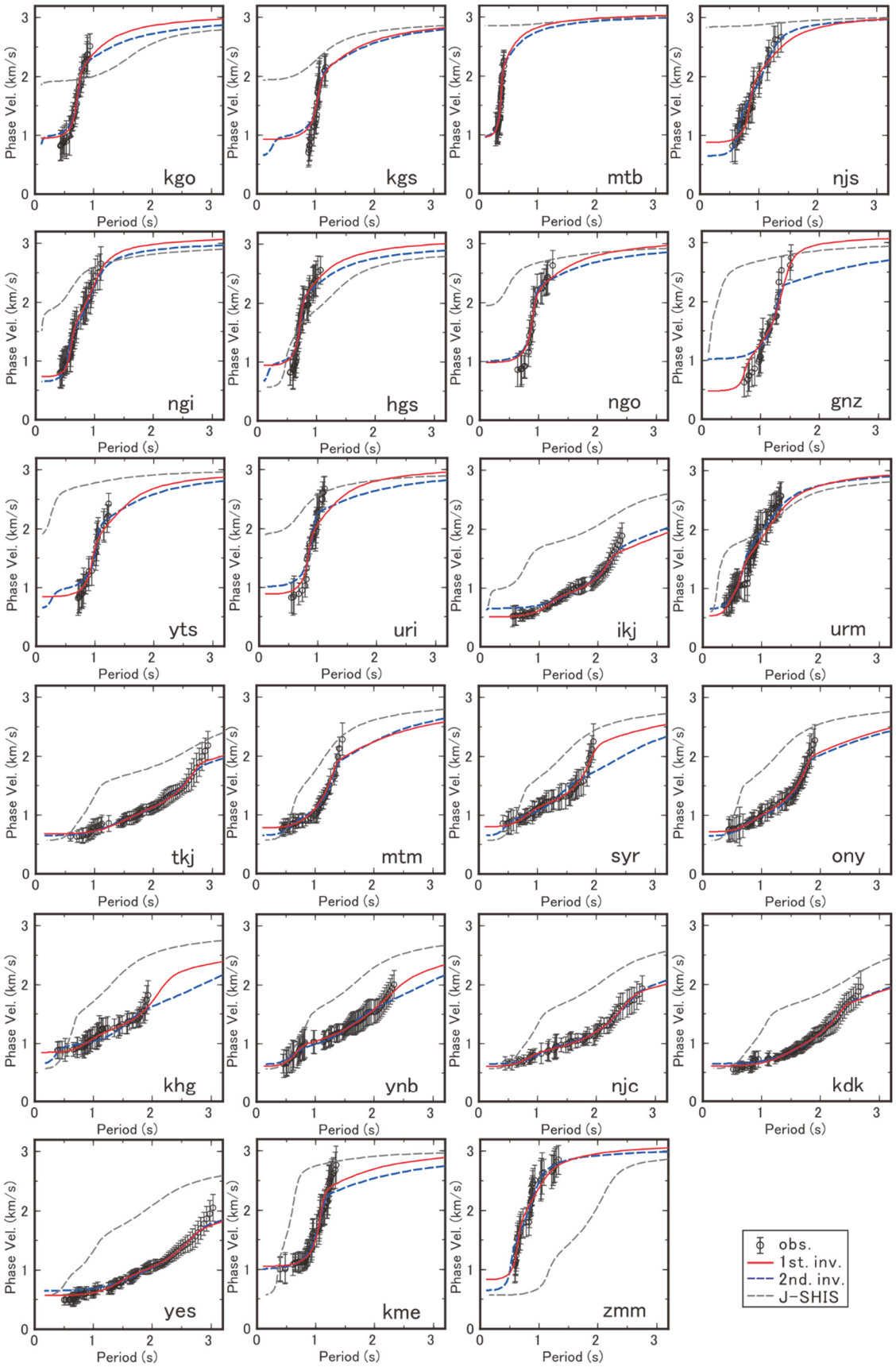

Fig. 7 Comparison of phase velocities

6. AVERAGE S-WAVE VELOCITY AND BOUNDARY DEPTH OF EACH LAYER

Many numerical models of the subsurface structure used in the simulation for ground motion evaluation, such as the finite difference method, model the medium properties uniformly inside each layer (e.g., the J-SHIS model[6]). Therefore, in this study, the average Vs value and the boundary depth of each layer are presented based on the results of Section 5 as information to facilitate the creation of a three-dimensional numerical model of the subsurface structure with the same number of layers and homogeneity within the layers. Because the velocity structure estimated in Section 5 was a four layer model at more than half of the sites, we treated it as four layers here as well, which is the maximum number of layers. As in Yamada and Takenaka[11], to obtain the average Vs value for each layer, the first, second, and third layers were weighted average by the layer thickness value, and the fourth layer was simply averaged by the Vs value. As shown in Table 4, Vs values less than 0.9 km/s were considered as layer 1, 0.9–1.6 km/s as layer 2, 1.6–2.5 km/s as layer 3, and more than 3.0 km/s as layer 4. The average values of Vs were 0.69, 1.10, 2.01, and 3.46 km/s for layers 1, 2, 3, and 4, respectively, as shown in Table 5a. Although some of the survey sites were located far from each other, it was possible to show the average S-wave velocity in the Okinawa Islands region. The average Vs values calculated for the Miyako and Yaeyama Islands (Sakishima Islands) shown by Yamada and Takenaka[11] were 0.69, 1.08, 1.74, and 3.44 km/s from the surface, as shown in Table 5b. Although there is a difference in the value of the third layer, the average Vs values for the two islands were similar. The number of layers is also the same, that is, four layers. Therefore, although the Okinawa Islands and the Sakishima Islands are approximately 300 km apart and have different surface geology, it is possible to set the same parameters for the engineering basement of Vs 0.5–0.7 km/s in layer 1 and the layer below it (layer 2) for both islands when considering the numerical model of the velocity structure.

Using the average value of Vs obtained, the layer thickness value at all sites was again calculated from the inversion, assuming a four-layer structure model. This result is called 2nd inv. The procedure of the inversion is the same as that described in Section 5; for the search range, the Vs value is fixed at the average value of the Okinawa Islands (Table 5a), as shown in Table 6, and the other parameters are the values shown in Table 3 (four-layer model). The obtained layer boundary depths are presented in Table 7. The theoretical phase velocity of the fundamental-mode Rayleigh wave estimated from the obtained velocity structure model is shown by the blue dotted line (2nd inv.) in Fig. 7. When the Vs value is fixed (2nd inv.), the phase velocity (Fig. 7) is close to that of the originally estimated model (1st inv.) in many cases, and error bars of the observed phase velocity (obs.) are within the range in most periods. The correspondence between the obs. and the 2nd inv. in Fig. 7 were not significantly worse. However, there is a difference in GNZ between the short- and long-period sides of the obs. and 2nd inv. in Fig. 7, suggesting that the local subsurface structure may have an effect, or that there is a problem in setting parameters such as Vs value and number of layers.

These results (Table 7) can show a regional trend in the velocity structure because the Vs values are constant from layer to layer. The results of Table 7 are shown in Fig. 8 for each survey line in Fig. 1b. According to the results, the variation in the layer boundary depth is less in the B line from northeast to southwest, whereas it is greater in the southern part of the A line connecting the northwest and southeast. The depth of the top of the seismic basement tends to be deeper from northwest to southeast, mainly in the southern part of Okinawa Island. It is about 0.5 km in the northern and western coastal areas of the island, whereas it is 2.0–2.5 km deep in the east coast area of the island. Although the depth values cannot be directly compared, this trend is similar to the trend of the boundary depth shown in the drilling in Fig. 2b. The thickness of the third layer in the northern part of Okinawa Island is very small.

Table 5 Average of the S-wave velocities

a) Okinawa Islands

Layer	Vs (km/s)
1	0.69
2	1.10
3	2.01
4	3.46

b) Miyako and Yaeyama Islands

Layer	Vs (km/s)
1	0.69
2	1.08
3	1.74
4	3.44

Table 6 Search range for re-inversion (2nd inv.) with fixed velocity value

Layer	Vs (km/s)	Th (km)	ρ (g/cm^3)
1	0.69	0.001–1.0	1.95
2	1.10	0.001–1.0	2.15
3	2.01	0.001–2.0	2.35
4	3.46	∞	2.60

Table 7 Layer boundary depth (in km) of the model (2nd inv.) obtained by the inversion with fixed Vs value

	KGO	KGS	MTB	NJS	NGI	HGS	NGO	GNZ	YTS	URI	IKJ	URM	TKJ	MTM	SYR	ONY	KHG	YNB	NJC	KDK	YES	KME	ZMM
1–2	0.03	0.08	0.02	0.22	0.16	0.05	0.01	0.00	0.08	0.01	0.41	0.14	0.39	0.18	0.14	0.21	0.11	0.19	0.31	0.44	0.46	0.01	0.17
2–3	0.35	0.53	0.19	0.23	0.24	0.37	0.45	0.55	0.52	0.40	1.06	0.36	1.14	0.61	0.66	0.75	0.75	0.79	1.08	1.04	1.19	0.46	0.18
3–4	0.48	0.57	0.20	0.23	0.24	0.39	0.47	0.87	0.54	0.60	1.60	0.37	2.30	0.90	2.07	1.37	2.46	2.37	2.21	2.07	2.52	0.80	0.19

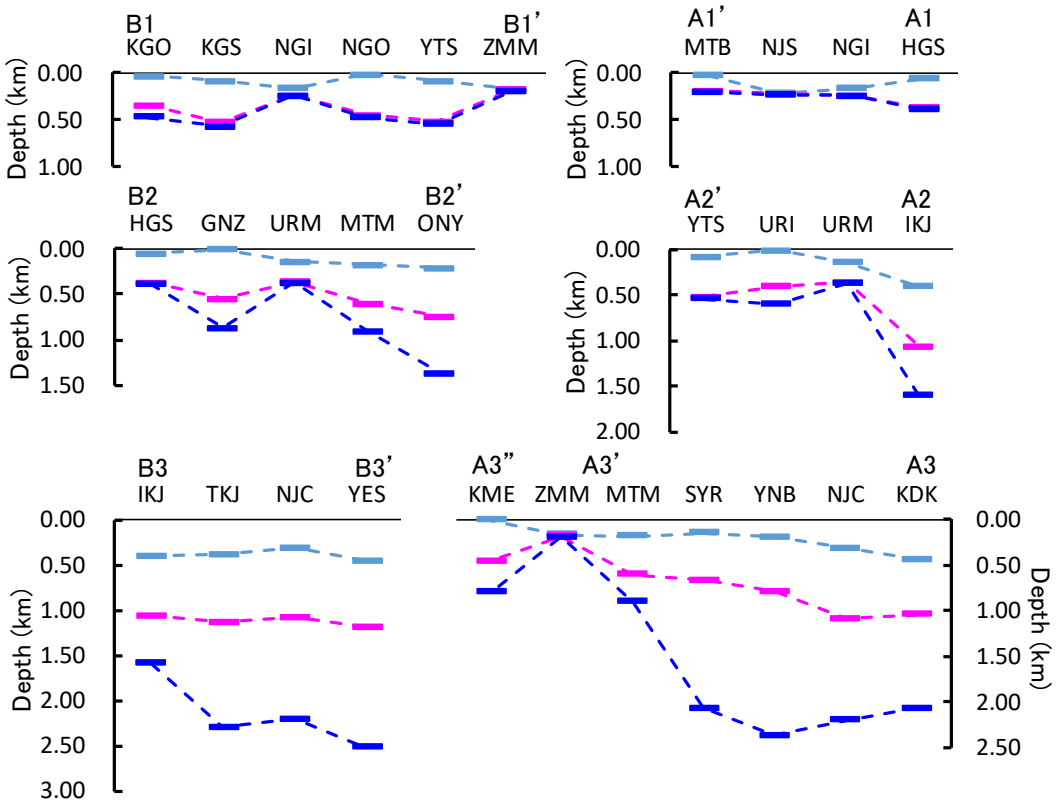

Fig. 8 Comparison of the layer boundaries for each survey line

7. CONCLUSION

In this report, we estimated the S-wave velocity structure to the layer equivalent to Vs 3 km/s using the records of microtremor array observations conducted at 23 sites in the Okinawa Islands. As a result, we could show the S-wave velocity structure of one to three layers above the seismic basement at each site, and the top depth of the one is 0.2–0.4 km in the northern and western Okinawa Island, and 2.0–2.5 km in the southern Okinawa Island. In the southern part of Okinawa Island, the slope ranges from northwest to southeast. The average Vs values of each layer and the depth of the layer boundary for the four-layer model are also shown, with values of 0.69, 1.10, 2.01, and 3.46 km/s. These results were similar to those of the Miyako and Yaeyama Islands and can be used as basic data for improving the S-wave velocity structure model.

In this study, we only showed the 1D velocity structure of each site. However, it is necessary to examine the validity of the obtained velocity structure information through, for example, 3D ground motion simulations that consider the seafloor and topography and improve and construct the structural model. The phase velocity in the band with a period less than 0.5 s and the subsurface structure of the surface soil shallower than the engineering basement (Vs less than 0.6 km/s) can be considered in evaluating the strong ground motion with accuracy and wider period band.

ACKNOWLEDGMENT

The microtremor array observations in this study were carried out with the cooperation of Dr. Masanao Komatsu of the Graduate School of Natural Science and Technology, Okayama University, and students of the Faculty of Science, Okayama University, the Graduate School of Science, Kyushu University, and the Faculty of Education, University of Teacher Education Fukuoka. GMT (Wessel and Smith[28]) was used to create the map. We would also like to thank the three anonymous reviewers and the editorial staff for their very careful review, which helped to improve this paper. Finally, Part of this work was supported by JSPS Grants-in-Aid for Scientific Research (B) 23310122 and 26282105. We would like to thank all those involved.

REFERENCES

1) The Headquarters for Earthquake Research Promotion: Regional Seismicity Okinawa (in Japanese, title translated by the authors). http://www.jishin.go.jp/regional_seismicity/rs_kyushu-okinawa/p47_okinawa/ (last accessed on February 11, 2021)
2) Fire and Disaster Management Agency: Detailed Disaster Information, Earthquake Near the Mainland of Okinawa, 2010 (in Japanese, title translated by the authors). https://www.fdma.go.jp/disaster/info/assets/post594.pdf (last accessed on February 11, 2021)
3) Nakamura, M., Akamine, Y., Hamagawa, K., Higa, Y. and Nakaza, E.: A Questionnaire Seismic Intensity on 2010 Okinawa Honto Kinaki Earthquake, 2010, *The Sesmological Society of Japan 2010 Fall Meeting*, P1–71 (in Japanese).
4) The Headquarters for Earthquake Research Promotion: National Seismic Hazard Maps for Japan, 2018 (in Japanese). https://www.jishin.go.jp/evaluation/seismic_hazard_map/shm_report/shm_report_2018/ (last accessed on February 11, 2021)
5) Kashima, S. and Ono, H.: A Study of the Problems and Characteristics Okinawa High Density Area Built after WW2 / Case Study on Mawashi District in Naha City, Okinawa Prefecture, *Transactions of AIJ. Journal of Architecture, Planning and Environmental Engineering*, Vol. 82, No. 731, pp.

115–122, 2017 (in Japanese).
6) National Research Institute for Earth Science and Disaster Resilience: Japan Seismic Hazard Information Station (in Japanese). http://www.j-shis.bosai.go.jp/ (last accessed on February 11, 2021)
7) Nishizawa, A., Kaneda, K., Oikawa, M., Horiuchi, D., Fujioka, Y. and Okada, C.: Variations in Seismic Velocity Distribution along the Ryukyu (Nansei-Shoto) Trench Subduction Zone at the Northwestern End of the Philippine Sea Plate, *Earth, Planets and Space,* Vol. 69, No. 86, 2017. https://doi.org/10.1186/s40623-017-0674-7
8) Nakae, S.: Stratigraphic Division of the Pre Neogene Basement Complex in Ryukyu Arc and Its Correlation to Southwest Japan, *Chisitsu News*, No. 633, pp. 11–21, 2007 (in Japanese).
9) Leroy, L. W.: Smaller Foraminifera from the Late Tertiary of Southern Okinawa, *Shorter Contributions to General Geology*, U. S. Government Printing Office, pp. F1–F53, 1964.
10) Okinawa Prefecture: Natural Gas Resources Development Study Report, 95 p., 2012 (in Japanese, title translated by the authors).
11) Yamada, N. and Takenaka, H.: Deep Subsurface S-wave Structure of Sakishima (Miyako and Yaeyama) Islands, Southwestern Japan, *Journal of Japan Association for Earthquake Engineering*, Vol. 18, No. 1, pp. 77–88, 2018 (in Japanese).
12) Geospatial Information Authority of Japan: Digital Map 50m Grid (Elevation) Nippon-3, 2000.
13) Shinjyo, R.: Geology and Its Development of the Ryukyu Island Arc: An Example of Geology of Okinawa Island, Central Ryukyus, *Journal of Japan Society of Civil Engineers, Series A2 Applied Mechanics*, Vol. 70, No. 2, pp. I_3–I_11, 2014 (in Japanese).
14) Geological Survey of Japan, National Institute of Advanced Industrial Science and Technology: Geomap Navi (in Japanese). https://gbank.gsj.jp/geonavi/ (last accessed on February 11, 2021)
15) Fukuda, O., Motojima, K., Ijima, S., Kino, Y., Suzuki, T., Ogawa, K., Suda, Y., Shimizu, M., Inoue, M., Goto, H., Maki, S., Natori, H. and Koma, T.: Natural Gas Resources of Ryukyu Islands — Preliminary Report by the 4th Phase Survey Team of G. S. J.—, *Bulletin of the Geological Survey of Japan*, Vol. 20, No. 2, pp. 19–42, 1969 (in Japanese).
16) Industrial Policy Division, Department of Commerce, Industry and Labor, Okinawa Prefecture, Prospecting Joint Venture: Report on the Exploratory Research Project for the Promotion of Natural Gas Resources, 121 p., 2014 (in Japanese, title translated by the authors).
17) Kato, S., Nemoto, Y. and Hou, J.: Natural Gases Dissolved in Water in the Southern Part of Okinawa-Jima, Okinawa Prefecture, Japan, *Journal of the Japanese Association for Petroleum Technology*, Vol. 81, No. 4, pp. 312–321, 2016 (in Japanese).
18) Katoh, K. and Goto, S.: Current Situation of Deep Drilling in Our Country 4, *Chishitsu News*, No. 286, pp. 24–29, 1978 (in Japanese, title translated by the authors).
19) Okinawa Natural Gas Research Group: The Treasure of the World, Southern Okinawa Main Island Gas Field, *Chishitsu News*, No. 213, pp. 34–46, 1972 (in Japanese, title translated by the authors).
20) Kato, S., Honda, T. and Omijya, K.: Petroleum Geology of the Nanjyo R1 Exploratory Well, Okinawa Prefecture, *Journal of the Japanese Association for Petroleum Technology*, Vol. 77, No. 1, pp. 86–95, 2012 (in Japanese).
21) Fukuda, W. and Nagata, S.: Blowout of the Gushigashira R1 Well, *Chishitsu News*, No. 276, pp. 1–17, 1977 (in Japanese, title translated by the authors).
22) Capon, J.: High-Resolution Frequency-Wavenumber Spectrum Analysis, *Proceedings of the Institute of Electrical and Electronics Engineers*, Vol. 57, pp. 1408–1418, 1969. https://www.doi.org/10.1109/PROC.1969.7278
23) Okada, H.: Method of Estimation the Subsurface Structure by Microtremor Use, *Geophysical Exploration Handbook*, The Society of Exploration Geophysics of Japan, pp. 203–211, 1998 (in Japanese).

24) Yamanaka, H. and Ishida, H.: Application of Genetic Algorithms to an Inversion of Surface-Wave Dispersion Data, *Bulletin of the Seismological Society of America*, Vol. 86, pp. 436–444, 1996.
25) Yamanaka, H. and Yamada, N.: Estimation of 3D S-wave Velocity Model of Deep Sedimentary Layers in Kanto Plain, Japan, Using Microtremor Array Measurements, *BUTSURITANSA*, Vol. 55, pp. 56–65, 2002 (in Japanese).
26) Yamanaka, H., Takemura, M., Ishida, H., Ikeura, T., Nozawa, T., Sasaki, T. and Niwa, M.: Array Measurements of Long-Period Microtremors and Estimation of S-Wave Velocity Structure in the Western Part of the Tokyo Metropolitan Area, *Zisin 2*, Vol. 47, pp. 163–172, 1994 (in Japanese).
27) Kitsunezaki, C., Goto, N., Kobayashi, Y., Ikawa, T., Horike, M., Saito, T., Kuroda, T., Yamane, K. and Okuzumi, K.: Estimation of P- and S- Wave Velocities in Deep Soil Deposits for Evaluating Ground Vibrations in Earthquake, *Japan Society for Natural Disaster Science*, Vol. 9, No. 2, pp. 1–17, 1990 (in Japanese).
28) Wessel, P. and Smith, W. H. F.: New, improved version of the Generic Mapping Tools released, *Eos, Transactions, American Geophysical Union*, Vol. 79, No. 47, p. 579, 1998. https://doi.org /10.1029/98EO00426

(Original Japanese Paper Published: August, 2019)
(English Version Submitted: February 20, 2021)
(English Version Accepted: April 12, 2021)